

## Atomic displacement free interfaces and atomic registry in SiO<sub>2</sub>/(1×1) Si(100)

Justin M. Shaw,<sup>a)</sup> N. Herbots, Q. B. Hurst,<sup>b)</sup> D. Bradley, R. J. Culbertson, and V. Atluri  
*Department of Physics and Astronomy, Arizona State University, Tempe, Arizona 85287-1504*

K. T. Queeney  
*Department of Chemistry, Smith College, Northampton, Massachusetts 01063*

(Received 14 November 2005; accepted 29 July 2006; published online 29 November 2006)

We use ion beam analysis to probe the structure and interface of ultrathin thermal oxide films grown on (1×1) Si(100) surfaces prepared using the Herbots-Atluri [U.S. patent No. 6,613,677 (Sept. 2, 2003)] wet chemical clean. We discover that these oxide layers are structurally registered with the substrate lattice with no interfacial structural disorder. Registry of Si atoms is most pronounced along ⟨111⟩ directions relative to the Si substrate, consistent with a β-cristobalite epitaxial phase. This structurally registered phase transitions to an amorphous structure approximately 2 nm from the interface. © 2006 American Institute of Physics. [DOI: 10.1063/1.2358835]

### INTRODUCTION

Si/SiO<sub>2</sub> interfaces exhibit a transition from an ordered Si crystal to the amorphous structure of SiO<sub>2</sub> with virtually no electrically active defects. Recent theoretical predictions reveal that a partially ordered oxide phase can exist within approximately 3 nm of the interface.<sup>1</sup> Ordered cristobalite-like crystallites and residual order within a thermal oxide layer grown on Si have been observed using x-ray diffraction,<sup>2–5</sup> and cristobalite phases have been reported in SiO<sub>2</sub> precipitates in Si matrices using microscopy.<sup>6,7</sup> However, previous reports of two-dimensional ordered oxide phase extending from the Si(100) interface<sup>8–10</sup> remain a source of controversy.<sup>11,12</sup> Most recently, order from an ultrathin Si layer in silicon-on-insulator (SOI) substrates was found to extend into a thermal oxide grown above it.<sup>13</sup> However, the ultrathin Si layer in that work is relatively pliable and ordering is not observed when the oxides grow on rigid Si substrates. In this work, a patented chemical process was used to produce ultrasMOOTH (1×1) Si(100) templates<sup>14–18</sup> and grow 1–4 nm thermal oxides. A combination of ion beam channeling, nuclear resonance, and damage versus incident beam dose analysis demonstrates that significant atomic registry and order are present in the thin 1–2 nm interphase oxide region. In addition, the scattering data are confirmed by IR spectroscopy.

### EXPERIMENT

We used 100 mm B-doped ultraflat Si(100) wafers with a resistivity of 10–14 Ω cm as substrates. The patented Herbots-Atluri wet chemical clean and passivation<sup>14</sup> were performed in a class-10 chemical hood especially designed for this process located in a class-100 clean room at Arizona State University. All chemicals used were General Chemical Corp. class-10 grade. Wafers were first immersed in

NH<sub>4</sub>OH:H<sub>2</sub>O<sub>2</sub>:H<sub>2</sub>O (1:1:4), the so-called SC1 solution, held at 80 °C for 10 min; immersed in a 2% HF solution at room temperature for 2 min; and immersed in HCl:H<sub>2</sub>O<sub>2</sub>:H<sub>2</sub>O (1:1:4), the so-called SC2 solution, held at 80 °C for 10 min. Wafers were rinsed after each step for 5 min in dry N<sub>2</sub> purged 18.3 MΩ de-ionized water. The surfaces were subsequently passivated with a 1 min dip in HF:methanol (1:10) and a final rinse in pure methanol. Further details of this process are described elsewhere<sup>14–18</sup> and this procedure results in a (1×1) ordered surface stable in ambient air.<sup>15,18</sup> The surfaces were oxidized using either a furnace or a rapid thermal oxidation system<sup>19</sup> strictly used for gate oxidation to reduce contamination.

Ion beam analysis (IBA) was performed on a 1.7 MV General Ionex Tandetron accelerator with a base pressure in the 10<sup>–8</sup> Torr range using a two axis goniometer capable of azimuthal and polar rotations of the sample. The signal-to-noise ratio for O is enhanced by a factor of approximately 230 relative to 2 MeV Rutherford backscattering spectrometry (RBS) by combining channeling with the 3.045 MeV <sup>16</sup>O(α,α)<sup>16</sup>O nuclear resonance analysis (NRA).<sup>20–23</sup>

Because of the narrow energy spread of 10 keV for the full width at half maximum of this resonance, the energy of the incident beam is calibrated prior to each measurement. To ensure accuracy, we conducted independent measurements of O areal density with conventional 1 MeV RBS with 3.045 MeV NRA for the thickest (4.5 nm) oxide layer used in this study. These two measurements yield identical values of O areal density well within the experimental error, indicating that the narrow resonance energy spread does not affect our measurements for oxide films thinner than 4.5 nm.<sup>15</sup>

The incident ion beam direction is aligned along the desired crystallographic direction for channeling analysis via systematic angular scans<sup>21,22</sup> for each sample. This alignment procedure is critical for an accurate quantitative analysis of the Si surface peak. Our sample goniometer is capable of rotations in two directions: azimuthal and polar. This requires us to perform two separate angular scans, one for each direction, to achieve proper alignment. In order to quantify

<sup>a)</sup>Present address: National Institute of Standards and Technology, Boulder, CO 80305; electronic mail: justin.shaw@nist.gov

<sup>b)</sup>Present address: Raytheon, Tucson, AZ 85744.

the error introduced into our measurement of the Si surface peak areal density using our alignment procedure, we performed a detailed study of the sensitivity of the Si surface peak on small misalignments and determined the error introduced into the measurement from our procedure and instruments. For the  $\langle 111 \rangle$  channel, we measured the error in the Si surface peak to be less than 5% if the incident beam alignment is within  $\pm 0.13^\circ$  of the  $\langle 111 \rangle$  channel for the sample azimuthal direction and  $\pm 0.25^\circ$  for the polar direction. Experimentally induced misalignment was experimentally measured to be at most  $\pm 0.06^\circ$  in both these directions and is due mostly to the goniometer mechanical precision. Thus, the error in the Si surface peak areal density due to experimental misalignment is at most 5%. Absolute values of O and Si areal densities are found using the standard surface approximation given the thickness of the oxide layers and the fact that the nuclear resonance occurs throughout the entire film and are given for O and the Si surface peak in Eqs. (1) and (2), respectively. Normalization is achieved from the Si signal height obtained from rotating random spectra.

$$(Nt)_O = \frac{A_O \sigma_{Si} N_{Si}}{H_{Si} \sigma_O [S]_{Si}} dE, \quad (1)$$

$$(Nt)_{SSP} = \frac{A_{SSP} N_{Si}}{H_{Si} [S]_{Si}} dE. \quad (2)$$

Here,  $(Nt)_O$  and  $(Nt)_{SSP}$  are the O and Si surface peak areal densities ( $\text{cm}^{-2}$ ), respectively,  $A_O$  and  $A_{SSP}$  are the O and Si surface peak signal integrated areas,  $H_{Si}$  is the rotating random Si signal height,  $\sigma_{Si}$  and  $\sigma_O$  are the RBS cross sections for Si and O, respectively,  $N_{Si}$  is the atomic density of Si,  $[S]_{Si}$  is the stopping power factor for  $\text{He}^{++}$  in Si, and  $dE$  is the energy per channel.

Even with the cross-section enhancement achieved by combining channeling with NRA, the error in absolute O areal density measured in individual channeling spectra is still too large for three reasons: (1) necessity of large incident beam doses for good measurement statistics in the O signal (these analyzing doses modify the structure of ordered films), (2) ion induced damage, and (3) ion assisted oxidation of the surface. We resolved this issue by taking a systematic sequence of channeling spectra with an increasing cumulative dose and analyzing the O and Si surface peak coverages for each sample as a function of the incident beam dose. The y intercept of a linear fit of the detected areal density versus dose yields an areal density measurement at zero incident beam dose, and thus, free of measurement artifacts. We call this technique the *damage curve* which we demonstrate and apply in more detail in Refs. 15–17. We have established in these works that the analyzing beam damage in thin ordered oxide films—as would be expected—increases linearly for the Si surface peak and O peak with increasing dose.

## RESULTS AND DISCUSSION

Damage curves for both the Si surface peak and O are measured along  $\langle 100 \rangle$ ,  $\langle 110 \rangle$ , and  $\langle 111 \rangle$  directions for oxide thicknesses ranging between 1 and 4 nm. The areal density measured for the Si surface peak in each film is shown as a

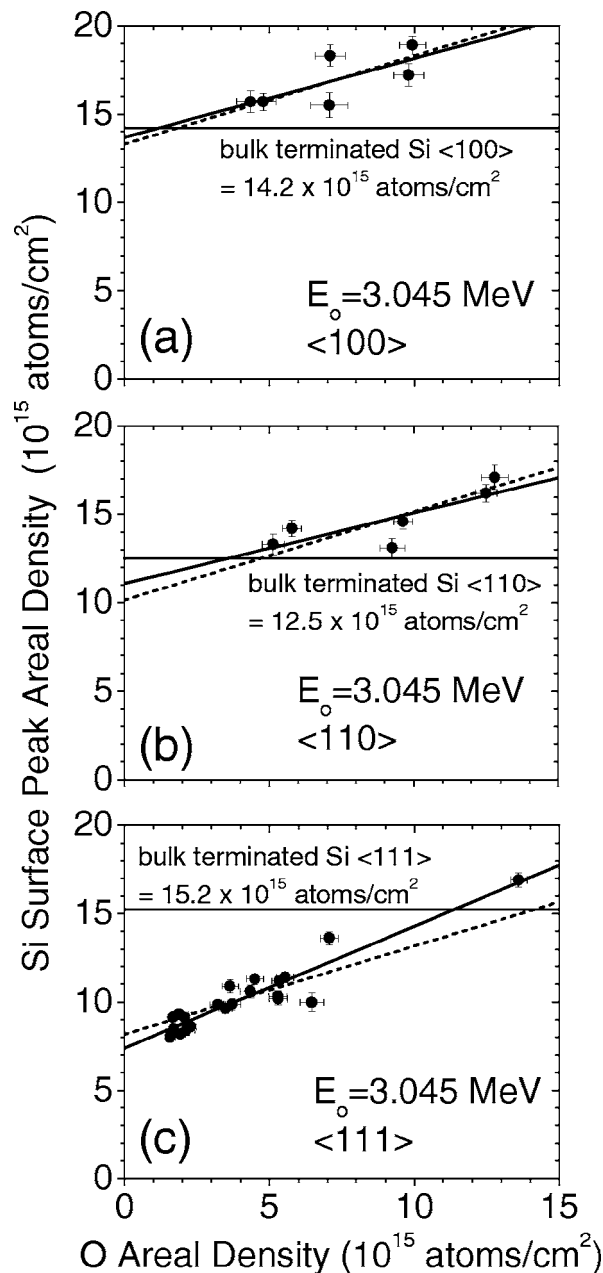


FIG. 1. Si surface peak areal density vs O areal density taken along the (a)  $\langle 100 \rangle$ , (b)  $\langle 110 \rangle$ , and (c)  $\langle 111 \rangle$  channels with corresponding regression fits. The dashed lines show regression fits with the slope fixed at the ideal value of 0.5. The horizontal line shows the bulk Si surface contribution.

function of the O areal density detected along the  $\langle 100 \rangle$  and  $\langle 110 \rangle$  directions in Figs. 1(a) and 1(b), respectively. In addition, the contribution of the bulk terminated Si to the total Si surface peak is drawn as a horizontal reference line throughout the plot to show how much of the surface peak is expected to intrinsically arise from the Si substrate independently of the surface structure and oxide film. The Si bulk contribution is calculated using Monte Carlo methods with the 3DSTRING computer code. The accuracy of these calculations at 3.045 MeV was confirmed by comparing the computed values by the same code for 1 and 2 MeV scatterings with previously reported computations by other groups.<sup>24–26</sup>

A linear regression fit of the  $\langle 100 \rangle$  and  $\langle 110 \rangle$  data in Figs. 1(a) and 1(b) yields a y-intercept value that matches that of

TABLE I. Comparison of values of net disorder along the  $\langle 100 \rangle$  and  $\langle 110 \rangle$  channels at the Si/SiO<sub>2</sub> interface among this work and previously reported works.

Channel	Incident ion energy (MeV)	Net disorder in Si ( $\times 10^{15}$ at. cm <sup>-2</sup> )	Equivalent disordered Si monolayers	Reference	Initial surface process
$\langle 100 \rangle$	3.045	-0.2	0.0	This work	Herbots-Atluri clean
	0.8	1.4	2.1	25	Not reported
	0.8	7.4	10.9	26	RCA
	0.8	6	8.8	26	HF in ethanol
	0.8	5.3	7.8	26	Rapid thermal cleaning
$\langle 110 \rangle$	3.045	-1	0.0	This work	Herbots-Atluri clean
	0.8	2.2	2.3	24	Aqueous HF
	0.8	2.2	2.3	25	Not reported

the calculated bulk Si in both cases. Linear regression fits are also included (dashed line) with the slope fixed at 0.5 (for an ideal 1:2 ratio of Si to O) and show only a small deviation in the  $y$  intercept. This indicates that the Si/SiO<sub>2</sub> interface is free from disorder within our small measurement errors, in contrast to the net disorder reported by other groups.<sup>24–26</sup> We use the same procedure as these other groups by taking the net interfacial disorder as the difference between the ideal bulk terminated calculated value and the  $y$  intercept of the linear fit of the measured values. Table I compares our results for the measured net interface disorder with previously published data from other groups using alternatively prepared oxides. The equivalent disorder in Si monolayers (MLs) at the interface ranges from 2.1 to 10.9 for previous works and is zero for this study.

Figure 1(c) shows the Si surface peak versus O areal density plot taken along the  $\langle 111 \rangle$  channel. We find that the  $y$  intercept of the linear regression line is significantly below that of the calculated bulk Si surface areal density along this direction. These data indicate that Si atoms in the substrate are being shadowed by Si atoms in the oxide layer. This can only occur if Si atoms in the oxide layer are registered with the atoms in the crystal structure of the Si substrate. In order to maintain such a registry within the interfacial phase, O atoms would have to be inserted along  $\langle 111 \rangle$  directions, suggesting a cristobalite-like phase. It would also explain the more pronounced shadowing effect we observe in the  $\langle 111 \rangle$  direction for Si atoms in the present work, as the insertion of O atoms between the Si bonds without disruption of their alignment would increase the shadow cone from one atom to the next. In addition, the effects of shadow cones in such a structure would not be pronounced along the  $\langle 100 \rangle$  and  $\langle 110 \rangle$  directions, consistent with our data for those directions. Finally, the fact that the Si surface peak yield increases with O coverage above two MLs indicates that registry and ordering are confined to an interphase region estimated to be 1–2 nm in thickness. This is due to the fact that an unordered structure will increase the Si surface peak yield more rapidly than an ordered structure. Most recently, Monte Carlo simulations of channeling along  $\langle 100 \rangle$ ,  $\langle 110 \rangle$ , and  $\langle 111 \rangle$  in ordered SiO<sub>2</sub>/Si(100) films and using the Moliere approximation to the Thomas-Fermi potential reveal that a 2 nm epitaxial  $\beta$ -cristobalite SiO<sub>2</sub> phase that transitions to an amorphous

structure above 2 nm matches the present IBA data along all three  $\langle 100 \rangle$ ,  $\langle 110 \rangle$ , and  $\langle 111 \rangle$  directions.<sup>27</sup> These simulations confirm, in particular, the effect of the geometry of the cristobalite structure upon the increase of magnitude of shadowing observed in the  $\langle 111 \rangle$  when compared to the  $\langle 110 \rangle$  and the  $\langle 100 \rangle$ . In addition the simulations demonstrate that the cristobalite is tetragonally distorted in order to align with the Si(100). The growth mode for these ordered SiO<sub>2</sub> films is thus one where an amorphous overlayer forms over a critical thickness instead of islanding.

To confirm by an independent technique the detection of atomic registry at the Si/SiO<sub>2</sub> interface, these oxides were characterized using a Fourier transform infrared (FTIR) spectroscopy technique developed specifically to study oxide interfacial regions.<sup>28,29</sup> Infrared absorption spectra are taken at incremental thicknesses as the oxide layer is gradually removed via a dilute HF solution. Longitudinal-optic (LO) and transverse-optic (TO) adsorption frequencies are shown as a function of oxide in Figs. 2(a) and 2(b), respectively, comparing the oxides prepared on Herbots-Atluri chemically cleaned surfaces (ordered) and oxides grown using conventional RCA clean prepared surfaces (control). Optical mode adsorption frequencies were found to be higher within the first 2.5 nm of the ordered oxides compared to the control oxides grown on surfaces cleaned with a traditional RCA. In addition, the optical absorption frequencies were found to be

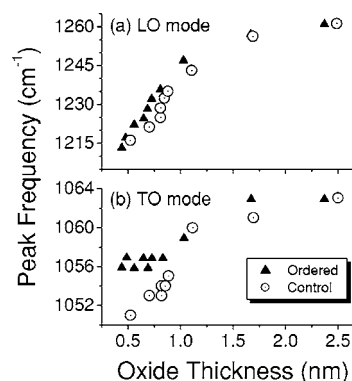


FIG. 2. FTIR measurements of the (a) LO and (b) TO modes for an oxide grown on a surface prepared with the Herbots-Atluri wet chemical clean (▲) (ordered) and on a traditional RCA clean prepared surface (○) (control) as a function of oxide thickness.

stable and well defined across the first 1.0 nm of the interface for the ordered oxides while the control oxides exhibit a progressive shift towards lower frequencies, consistent with disorder. These data provide further confirmation that our oxides have a well defined structure across the interface with a unique coordination and stoichiometry.

## SUMMARY

In conclusion, we have detected significant atomic registry in an interfacial phase or interphase between Si and SiO<sub>2</sub> by forming ultrathin oxides nucleated on a patented OH-terminated (1 × 1) Si(100) surface<sup>14–18</sup> by combining ion beam channeling, NRA, and a damage curve analysis. This innovative method maximizes the signal-to-noise ratio and removes artifacts from ion beam damage and ion beam induced oxidation. We observe significant shadowing in the ⟨111⟩ direction and zero interfacial disorder along the ⟨100⟩ and ⟨110⟩ directions. This phase consists of a 2 nm epitaxial β-cristobalite structure above which amorphous oxide forms. FTIR measurements confirm the presence of an ordered oxide interphase region.

## ACKNOWLEDGMENTS

The authors are grateful for the technical assistance of Barry Wilkens in the IBeAM facility at Arizona State University, Brian Doyle and Gang Bai at Intel Corp. for use of their facilities, and financial support from Intel Corp. under Grant No. ASUF133-1220 and the Research Corporation under Grant No. RA0256.

<sup>1</sup>J. C. Phillips, *J. Vac. Sci. Technol. B* **17**, 1803 (1999).

<sup>2</sup>I. Takahashi, T. Shimura, and J. Harada, *J. Phys.: Condens. Matter* **5**, 6525 (1993).

<sup>3</sup>P. H. Fuoss, L. J. Norton, S. Brennan, and A. Fischer-Colbrie, *Phys. Rev. Lett.* **60**, 600 (1988).

<sup>4</sup>K. Tatsumura, T. Watanabe, D. Yamasaki, T. Shimura, M. Umeno, and I. Ohdomari, *Phys. Rev. B* **69**, 085212 (2004).

<sup>5</sup>M. Castro-Colin, W. Donner, S. C. Moss, Z. Islam, S. K. Sinha, and R. Nemanich, *Phys. Rev. B* **71**, 045311 (2005).

<sup>6</sup>S. Hahn, F. A. Ponce, W. A. Tiller, V. Stojanoff, D. A. P. Bulla, and W. E. Castro, *J. Appl. Phys.* **64**, 4454 (1988).

<sup>7</sup>S. Mahajan, G. A. Rozgonyi, and D. Brasen, *Appl. Phys. Lett.* **30**, 73 (1977).

<sup>8</sup>A. Munkholm, S. Brennan, F. Comin, and L. Ortega, *Phys. Rev. Lett.* **75**, 4254 (1995).

<sup>9</sup>A. Ourmazd, D. W. Taylor, J. A. Rentschler, and J. Beuk, *Phys. Rev. Lett.* **59**, 213 (1987).

<sup>10</sup>G. Renaud, P. H. Fuoss, A. Ourmazd, J. Bevk, B. S. Freer, and P. O. Hahn, *Appl. Phys. Lett.* **58**, 1044 (1991).

<sup>11</sup>T. Shimura, M. Umeno, I. Takahashi, and J. Harada, *Phys. Rev. Lett.* **79**, 4932 (1997).

<sup>12</sup>G. Y. Fan, J. M. Cowley, and J. C. H. Spence, *Phys. Rev. Lett.* **58**, 282 (1987).

<sup>13</sup>E.-C. Cho, M. A. Green, J. Xia, R. Corkish, and A. Nikulin, *J. Appl. Phys.* **96**, 3211 (2004).

<sup>14</sup>N. Herbots, V. Atluri, J. Xiang, J. D. Bradley, S. Banerjee, and Q. B. Hurst, U.S. patent No. 6,613,677 (Sept. 2, 2003).

<sup>15</sup>N. Herbots, J. M. Shaw, Q. B. Hurst, M. P. Grams, R. J. Culbertson, D. J. Smith, V. Atluri, P. Zimmerman, and K. T. Queeney, *Mater. Sci. Eng., B* **87**, 303 (2001).

<sup>16</sup>Q. B. Hurst *et al.*, *Mater. Res. Soc. Symp. Proc.* **567**, 183 (2000).

<sup>17</sup>N. Herbots, V. Atluri, Q. Hurst, J. M. Shaw, S. Banerjee, J. D. Bradley, R. J. Culbertson, and D. J. Smith, *Mater. Res. Soc. Symp. Proc.* **510**, 157 (1999).

<sup>18</sup>V. Atluri, Ph.D. thesis, University of Arizona, 1998.

<sup>19</sup>Oxidation and electrical characterizations were performed at the R1 facility, Intel Corp., Santa Clara, CA.

<sup>20</sup>V. Atluri, N. Herbots, D. Dagel, S. Bhagvat, and S. Whaley, *Nucl. Instrum. Methods Phys. Res. B* **118**, 144 (1996).

<sup>21</sup>L. C. Feldman, J. W. Mayer, and S. T. Picraux, *Fundamentals of Surface and Thin Film Analysis* (North-Holland, New York, 1986).

<sup>22</sup>L. C. Feldman and S. T. Picraux, *Materials Analysis by Ion Channeling* (Academic, New York, 1982).

<sup>23</sup>J. A. Leavit, L. C. McIntyre, Jr., M. D. Ashbaugh, J. G. Oder, Z. Lin, and B. Dezfouly-Arjomandy, *Nucl. Instrum. Methods Phys. Res. B* **44**, 260 (1990).

<sup>24</sup>N. Cheung, L. C. Feldman, P. J. Silverman, and I. Sternsgaard, *Appl. Phys. Lett.* **35**, 859 (1979).

<sup>25</sup>T. E. Jackman, J. R. MacDonald, L. C. Feldman, P. J. Silverman, and I. Sternsgaard, *Surf. Sci.* **100**, 35 (1980).

<sup>26</sup>F. C. Stedile, I. J. R. Baumvol, I. F. Oppenheim, I. Trimaille, J.-J. Ganem, and S. Rigo, *Nucl. Instrum. Methods Phys. Res. B* **118**, 493 (1996).

<sup>27</sup>D. Bradley, Ph.D. thesis, Arizona State University, 2006; See also D. Bradley, R. J. Culbertson, N. Herbots, J. Shaw, and V. Atluri, *Appl. Phys. Lett.* (to be submitted).

<sup>28</sup>K. T. Queeney, M. K. Weldon, J. P. Chang, Y. J. Chabal, A. B. Gurevich, J. Sapjeta, and R. Lopila, *J. Appl. Phys.* **87**, 1322 (2000).

<sup>29</sup>K. T. Queeney, N. Herbots, J. M. Shaw, V. Atluri, and Y. J. Chabal, *Appl. Phys. Lett.* **84**, 493 (2004).